Evolution of circumbinary protoplanetary disks with photoevaporative winds Due to External Far Ultraviolet Radiation

mmshadmehri[1], Sayyed Masoumeh Ghoreyshi[1], and nak$_6$455[1]

[1]Affiliation not available

June 20, 2018

Abstract

Lifetime of the protoplanetary disks (PPDs) are beleived to be severely constrained by material depleting mechanisms, including photoevaporative winds due to the internal or external radiation sources. Most previous studies focused on exploring role of the winds in the exposed PPD with a single star, however, exploring evolution of the circumbinary disks with phtoevaporative winds due to external radiation sources deserve further investigation. In this study, we follow evolution of circumbinary PPDs with photoevaporative winds due to the external far ultraviolet (FUV) radiation field. We show that this mass losing process severely constrain a PPD properties, including its lifetime, mass and radius. Lifetime of a circumbinary PPD, for instance, is found to be a factor of about 2 longer than a circumstellar analogue. We find that this value strongly depends on the viscosity parameter. **To be completed ...**

m.shadmehri@gu.ac.ir (MS) *Iran Science Elites Federation postdoctoral fellow

1   Introduction

Text....Dr Ghoreyshi

Text...Dr Alipor

Text...Dr Shadmehri

Since the planet formation time-scale should not exceed lifetime of the protoplanetary disks (PPDs), constraining their lifetime plays an essential role in the current theories of planet formation (for recent reviews, e.g., Armitage, 2011; Ercolano and Pascucci, 2017). Magnetically-driven winds (Blandford and Payne, 1982) or photoevaporative mechanisms (e.g., Alexander et al., 2006; Gorti et al., 2009) and mass accretion onto the central star or already formed planets are efficient mass depletion processes that will eventually lead to a PPD dispersal. The relative importance of these mass-loss processes, however, strongly depends upon a PPD physical properties. While magnetized winds are known to be effective at the inner region of a PPD, photoevaporation due to the radiation field of the central star (e.g., Alexander et al., 2006; Gorti et al., 2009) or its ambient stars are efficient at the outer part (Anderson et al., 2013). Current theoretical models suggest that PPDs lifetime is less than ??. Furthermore, properties of the molecular cloud cores within which PPDs are thought to be formed can dramatically impact PPDs lifetime. (Li and Xiao, 2016; Xiao and Chang, 2018).

The mass-loss due to the radiation field from the central star or external sources, as evaporative agents in disk erosion, is a key quantity in constructing disk models with the photoevaporative winds. Primary focus of most previous studies was to elaborate role of the internal sources, including X-ray (e.g., Owen et al., 2010a, 2011a) and UV-radiation (e.g., Alexander et al., 2006), in the dispersal of PPDs where are

in the isolated areas. But PPDs residing in populated regions that contain OB stars are exposed to their ambient radiation field too. (Anderson et al., 2013) (hereafter; AAN2013) studied evolution of a viscous disc with photoevaporation due to far ultraviolet (FUV) radiation flux from external stars using existing photoevaporative models. In order to explore the relative importance of the internal and externals radiation fields in disk erosion, they also considered X-ray photoevaporation due to the host star and found that external sources are dominant in the dispersal of a PPD with a solar-mass host star. A PPD lifetime, its mass and radius, therefore, are constrained severely due to the external FUV radiation field (AAN2013).

Following recent discoveries of the circumbinary planets (Doyle et al., 2011; Orosz et al., 2012; Schwamb et al., 2013), there is a growing interest to understand evolution of the circumbinary PPDs. Theoretical attempts to model circumbinary discs, however, started decades before recent discovery of the circumbinary discs mostly motivated by ?. Following lines of the standard disc model (Shakura and Sunyaev, 1973), various circumbinary disk models with incorporating the binary torque have been developed over recent years (e.g., Martin et al., 2013). Numerical models ??. (Rosotti and Clarke, 2018) studied evolution of the discs around components of a binary system with photoevaporation by X-rays from the respective star.

(Vartanyan et al., 2016) developed a circumbinary disk model without winds to explore its steady-state structure and evolution via analytical and numerical solutions. Their analysis showed that binary torque at the inner edge has a profound effect on the disk structure at all radii. They showed a circumbinary disk evolves with a significantly reduced accretion rate at its inner edge in comparison to a similar disk with a single star. A circumbinary disk, therefore, evolves on a longer time-scale in comparison to a cicumstellar disk counterpart.

In the light of this finding and prominent role of photoevaporative winds in shortening a disk lifetime, it is worthwhile exploring structure of a circumbinary disk in the presence of this mass-losing process. This problem has been addressed by (Alexander, 2012) who studied evolution of a circumbinary disk with photo-evaporative winds due to the radiation field of the host star. (Alexander, 2012) found that a circumbinary disk evolves with a larger surface density comparing to a disk counterpart with a single star. But he did not quantified disk lifetime, its mass and radius. (Alexander, 2012) primarily studied role of the *internal* radial field in a circumbinary disk erosion, whereas we plan to investigate constraints on a circumbinary PPD quantities due to the *external* radiation field which is a dominant evaporative source in the disks with a solar-mass host star according to AAN2013. We, therefore,

2   Basic Equations

A circumbinary PPD is modeled as a thin disk with a binary system at its center. Orbital plane of the binary with the primary and the secondary masses $M_{\rm p}$ and $M_{\rm s}$ and the semimajor axis $a_{\rm b}$ is assumed to be coplanar with the disk. The mass ratio of the binary components is $q \equiv Ms/Mp \leq 1$. Although the disk is subject to a time varying gravitational potential due to the binary orbital motion, as an approximation, we assume that the disk is rotating in the potential arising from the total mass, i.e., $M_{\rm c} = M_{\rm p} + M_{\rm s}$. Disk rotation profile, therefore, is Keplerian with the angular velocity $\Omega = (GM_{\rm c}/r^3)^{1/2}$. All disk quantities, furthermore, are assumed to be dependent only on the radial distance r and time t.

Under theses circumstance and following the standard approach for constructing a thin disk model (Shakura and Sunyaev, 1973), the surface density evolution equation for a circumbinary disk in the presence of the wind mass-loss is

$$\frac{\partial \Sigma}{\partial t} = \frac{1}{r}\frac{\partial}{\partial r}\left[3r^{1/2}\frac{\partial}{\partial r}\left(\nu \Sigma r^{1/2}\right) - \frac{2\Lambda\Sigma}{\Omega}\right] - \dot{\Sigma}_{\rm w}.$$

(1)

where ν is the turbulent viscosity and Λ is the specific angular momentum injection rate by the binary. Rate of the wind mass-loss is denoted by $\dot{\Sigma}_\mathrm{w}$. If the angular momentum injection rate set to be zero and wind mass-loss is neglected, the above equations reduces to the surface density evolution equation for a disc surrounding a single star. In the presence of the wind, i.e. $\dot{\Sigma}_\mathrm{w} \neq 0$, the equations describes a disc with wind mass-loss around a single star. Our focus, instead, is to explore evolution of a circumbinary disk with wind mass-loss. In doing so, we have to specify three important quantities.

The first key quantity is the turbulent viscosity ν, where its functional dependence on the disk quantities is defined in an ad-hoc fashion within the framework of the standard disk model. Disk turbulence is thought to be driven by the fluid instabilities, including magnetorotational instability (MRI; Balbus and Hawley, 1991) or gravitational instability, depending upon the disk properties. While a PPD inner region is subject to MRI as the main source of the turbulence, the outer part of a massive enough PPD is gravitationally unstable. Although describing turbulence in terms of an effective viscosity is a very simplified approach due to non-linear and chaotic nature of this complex phenomenon, in the standard thin disc model all these complexities are baypassed when the azimuthal-radial component of the stress tensor is assumed to be proportional to the pressure. This approach leads to a commonly used relation for the turbulent viscosity, i.e. $\nu = \alpha c_s^2 / \Omega$, where $\alpha < 1$ and c_s are the viscosity parameter and the sound speed respectively. The sound speed is written in terms of the disk midplane temperature T, i.e. $c_s = \sqrt{k_\mathrm{B} T / \mu}$ where k_B is the Boltzmann constant and $\mu = 2.1\ \mathrm{m_H}$ is the mean molecular weight and $\mathrm{m_H}$ is hydrogen mass. We considered power-law relation for temperature and we not used energy balance equation for disk. so, $T = T_0 (\frac{r}{r_0})^{-s}$. In this work, we assume that T_0 defined as the disk midplane temperature at a distance $r_0 = 1\mathrm{AU}$ is 300 K.

The second key quantity is the rate of angular momentum injection by the binary to the disk at radius r per unite disk mass, i.e., $\Lambda(\mathrm{cm^2 s^{-2}})$. Although the angular momentum injection is restricted to a narrow anulus at the inner region of a disc and the function rapidly decreases with the distance, the injected angular momentum at the disc inner edge is able to affect global structure of a disc. If the mass ratio q is not very small this torque can clears out a cavity in the disk center. The radius of cavity depends on the binary separation (MacFadyen and Milosavljević, 2008) and on the binary eccentricity (Pelupessy and Portegies Zwart, 2013). The tidal torque from the binary is defined as (Armitage and Natarajan, 2002)

$$\Lambda(r) = \mathrm{sgn}(r - a_b) \frac{f q^2 G M_c}{2r} \left(\frac{a_b}{\Delta_\mathrm{p}}\right)^4, \tag{2}$$

where f is a dimensionless normalization factor. Here, Δ_p is defined by $\Delta_\mathrm{p} = \max(H, r - a_b)$ where H is the disk scale height.

The third key quantity is the wind mass-loss rate, i.e., $\dot{\Sigma}_\mathrm{w}$. Its mechanism is commonly attributed to the magnetically or photoevaporative mechanisms. When a disk is exposed to a strong radiation field, this photoevaporative process leads to a significant disk mass removal. Source of radiation, however, is either the host star or ambient radiation field. When photoevaporative wind is due to the host star radiation, the mass-lose rate is (Hollenbach et al., 1994) PLEASE cite original work for the following relation.

$$\dot{\Sigma}_\mathrm{w} = \frac{\dot{M}}{4\pi r_g^2} \left(\frac{r}{r_g}\right)^{-5/2}, \tag{3}$$

where $\dot{M}$ the integrated mass-loss rates ARE YOU sure it is the mass-loss rate?!! Perhaps it is accretion rate. PLEASE CHECK. YES, it is mass-loss rate from wind. and r_g is a critical radius at which the heated gas becomes unbound from the disk. This critical radius, therefore, is defined as a radial distance where the sound speed becomes comparable to the escape velocity. For X-ray photoevaporation from host star, we have $r_g = 5.0\mathrm{AU}$ and $\dot{M} = 1.0 \times 10^{-8} M_\odot yr^{-1}$ (Owen et al., 2010b, 2011b).

Following models of (Adams et al., 2004) and AAN2013, the mass-lose rate due to FUV evaporation by the external stars is written as

$$\dot{\Sigma}_{\mathrm{w}} = \frac{Cn_{\mathrm{d}}\sqrt{k_{\mathrm{B}}T'\mu}}{4\pi}\left(\frac{r_g}{r}\right)^{\frac{3}{2}}\left[1+\frac{r_{ge}}{r}\right]\exp\left(-\frac{r_{ge}}{2r}\right), \tag{4}$$

where C is a constant of order unity and $n_d \approx 10^4 - 10^8 \mathrm{cm}^{-3}$ is the gas particle density at the disk edge (at r_d) (Adams et al., 2004). Outer edge or inner edge?? Here, T' is the temperature of the heated gas at r_g. For a radiation field strength $G_0 = 300$, r_{ge} is 157 AU (Adams et al., 2004). To calculate T', we use definition of r_g. This radius is

$$r_g = \frac{GM_{\mathrm{c}}\mu}{k_{\mathrm{B}}T'} \approx 226\mathrm{AU}(\frac{M_{\mathrm{c}}}{M_\odot})(\frac{T'}{1000})^{-1}. \tag{5}$$

So, r_{ge} is 157 AU corresponding to $T' = 1439.5$K. According to findings (Adams et al., 2004), this value of T' corresponds to the number density $n_d \approx 10^6 \mathrm{cm}^{-3}$. Comparisons of disc evolution with single and binary stars in the presence of external photoevaporation are then presented.

3   analysis

We solve surface density evolution equation (1) subject to boundary conditions ? and ? introduced by(Martin et al., 2013). An implicit finite difference method is adopted.We used 198 grids logarithmically with a grid inner boundary in $R_{in} = 1$AU and grid outer boundary $R_{out} = 20000$AU.The first,we ran for ..... to ensure get correct answer. Also, we have checked conserving angular momentum with this cod. Initial disk mass is fixed at $M_{\mathrm{d}0} = 0.1$ $\mathrm{M}_\odot$ and the initial surface density distribution is given by an exponentially truncated profile (e.g., Lynden-Bell and Pringle, 1974)

[ ]

$$\Sigma(r,0) = \frac{M_{\mathrm{d}0}}{2\pi(\exp(-\frac{5a_{\mathrm{b}}}{r_{\mathrm{d}0}})-e^{-1})r_{\mathrm{d}0}r}\exp(-r/r_{\mathrm{d}0}), \ r > 5a_{\mathrm{b}}. \tag{6}$$

where $r_{\mathrm{d}0}$ is the initial disk radius. Such an exponential form of the initial density was used by many authors (e.g., Alexander, 2012; Martin et al., 2013). One should note that, however, its coefficient is well adopted. For example, when the Alexander's equation of the initial surface density is integrated, the assumed initial disk mass is not obtained (Alexander, 2012). His incorrect coefficient leads to less initial mass and therefore shorter age.

For the circumstellar case, the boundary conditions (BCs) are described as (Vartanyan et al., 2016)

$$\frac{\partial F_J}{\partial l}|_{\mathrm{r_{in}}} = \frac{F_J(r_{\mathrm{in}})}{l_{\mathrm{in}}}, \ \frac{\partial F_J}{\partial l}|_{\mathrm{r_{out}}} = 0, \tag{7}$$

For the circumbinary case, however, the binary torque at inner boundary is strong and there is no material here. So, we assume that the surface density at inner boundary is zero. At the outer edge, we set radial velocity boundary equal to zero (Martin et al., 2013). So, we can write

$$\Sigma(r,t)_{\mathrm{r_{in}}} = 0, \frac{\partial F_J}{\partial l}|_{\mathrm{r_{out}}} = 0, \tag{8}$$

AAN2013 or Martin??AAN2013 used standard boundary conditions (BCs), where the surface density tends to be zero at the inner edge r_{in} and the disk can expand freely at the outer radius. A large outer boundary

for our computation domain is adopted, i.e.$r_{\text{out}} = 20000$ AU. In VGR2015, however, the following BCs are implemented:

$$\frac{\partial F_J}{\partial l}\big|_{\text{r}_{\text{in}}} = \frac{F_J(r_{\text{in}})}{l_{\text{in}}}, \frac{\partial F_J}{\partial l}\big|_{\text{r}_{\text{out}}} = 0, \tag{9}$$

where F_J is the viscous angular momentum flux defined as $F_J = 3\pi\nu\Sigma l$ and l is the specific angular momentum. In a circumstellar disk profile of F_J rapidly converge to $r^{1/2}$, whereas in a circumbinary disk F_J behavior tends to a flat distribution due to exerted binary torque at the inner edge. This interesting feature, however, is derived in the absence of winds. We can ran simulations with BCs used by AAN2013 or VGR2015, however, we prefer to implement those BCs introduced by VGR2015 with a mechanism of mass depletion. our goal is to explore circumbinary disk evolution with winds. Since VGR2015 studied circumbinary disc evolution subject to

To illustrate differences in a circumstellar disc evolution due to imposing the above BCs, we first perform evolution calculation for circumstellar disks using standard BCs used by AAN2015 and VGR2015.

Before presenting our results, it is more convenient to insure that our simulations are accurate in obtaining previous studies. To that purpose, we have recovered VGR2015 results for the circumbinary discs and findings of AAN2013 for a circumstellar disc orbiting a single star.

Our imposed boundary conditions, however, are different from those used by AAN2013 for a circumstellar disc. Figure 3 displays a circumstellar disc quantities corresponding to the BCs used by AAN2013 (dashed curves) and by (Vartanyan et al., 2016) (solid curves). The host star mass is fixed at $M = 1$ M$_\odot$. The initial disc mass and the initial disc radius are $M_{\text{d}} = 0.1 M_\star$ and $r_{\text{d}} = 30$AU, respectively. Other model parameters are $\alpha = 0.01$, $s = \frac{1}{2}$, $r_g = 157$AU, $T' = 1439.5$K and $n_d = 10^6\text{cm}^{-3}$. One can see that the disk age is shorter for the BCs used by AAN2013.

On the top left-hand panel, surface density profile of a disc including external wind is shown for different times, as labeled. Solid and dashed curves are corresponding to the solutions with BCs of AAN2015 and VGR2015 respectively. The initial surface density distribution is shown by a dotted curve. The adopted input parameters are $\alpha = 0.01$, $r_{\text{in}} = 0.05$ AU,$s = \frac{1}{2}$ IS THERE any other input parameters to bring here?. On the top right-hand panel, disk radius as a function of time is shown. On the bottom row, profiles of the disk mass (left) and evolutionary track in the plane of disk mass and radius (right) are shown for the presented solutions.

Figure 2 depicts surface density distribution (left) and the corresponding F_J profile for a circumbinary disk with photoevaporative wind due to external FUV radiation (solid curve) and without wind (dashed curve). Different colors correspond to different epochs, as labeled. The total mass of the primary and secondary stars with mass ratio $q = 1$ is $M = 1$ M$_\odot$. The binary separation is assumed to be $a_{\text{b}} = 0.2$ AU and, thereby, the inner edge becomes $r_{\text{in}} \simeq 2a_{\text{b}} = 0.4$ AU. Other model parameters are $\alpha = 0.01$, ... Reduction of the surface density with time is due to the viscous stresses, however, this reduction is more pronounced when externally photoevaporative wind is included. Disk spreading in the absence of the wind is pronounced, however, photoevaporative winds strongly deplete outer regions and create a sharp outer edge.

A disk lifetime is set by the time that it losses 99 percent of its initial mass.

Role of the viscosity parameter α on a circumbinary disk evolution is explored in Figure 4 by considering different values of this parameter, as labeled. Other model parameters are $a_{\text{b}} = 0.2 AU$, $q = 1$ and $f = 1$. On the top panel, disk mass as a function of time is shown. We find that disk lifetime strongly depends on the adopted viscosity coefficient. A disk can survive over a longer time period if a lower viscosity coefficient is considered. A key feature of the viscous disk evolution is its extension to the larger radii due to the angular momentum transport. A higher viscosity coefficient, therefore, implies that disk material transport to the large radii to occur faster. Photoevaporative winds on the other hand are more efficient at a disk outer

6

figures/f1/f1-eps-converted-to.pdf

Figure 1: On the top left-hand panel, surface density profile of a disk including external wind is shown for different times, as labeled.

region. In a disk with a large viscosity coefficient, since the gas reaches to the outer part over a shorter time period,
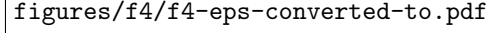
We have drawn figure 7 to show the effect of temperature in the circumbinary. That show that with increasing s to $s = 1$ (in other word decreasing power) disk lifetime increase almost 1.5 times than $s = \frac{1}{2}$ and $s = \frac{3}{7}$. So, with decreasing temperature disk lifetime increase. Figure 8 display the difference between the internal and external winds. Solid cure is external wind and dashed line is internal wind. this shows that the effect external wind is more than internal wind. In the case of external wind, lifetime disk are depleted quickly but the presence internal wind disk lifetime is more slowly and survive longer than external wind.

Figure 2: Profiles of the surface density (left) and the viscous angular momentum flux (right) for a circumbinary disk at different times, as lebeled. Masses of the primary and secondary stars are $M_\mathrm{p} = M_\mathrm{s} = 0.5$ $\mathrm{M}_\odot$ and their separation is taken to be $a_\mathrm{b} = 0.2$ AU. [ ]In this figure, we have $f = 1$ and $\alpha = 0.01$, $s = \frac{1}{2}$ Input parameters ? ... The circumbinary disk evolution with winds are displayed by solid curves, whereas solutions without winds are shown by dashed curves.
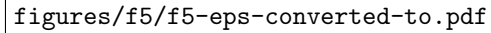
figures/f3/f3-eps-converted-to.pdf

Figure 3: Physical quantities of a circumbinray disk (solid curves) and an identical single-star disk (dashed curves). Total mass of the binary is $M_c = 1$ M$\odot$ and separation of its components is assumed to be $a_{\mathrm{b}} = 0.2$ AU. Other model parameters are $s = \frac{1}{2}$, $q = 1.0$, $\alpha = 0.01$, and $f = 1.0$. On the top left-hand panel, surface density distribution is shown at different ephocs, as labeled. On the top right-hand panel, disk radius is shown through time. On the bottom left-hand panel, disk mass as a function of time is shown. On the bottom right-hand panel, the locus of points in the plane of disk mass and radius corresponding to the explored cases are shown.

figures/f4/f4-eps-converted-to.pdf

Figure 4: The circumbinary disk mass (top), its radius (middle) and the corresponding track in the disk mass and radius plane (bottom) are shown for different values of the viscosity parameter, as labeled. The input parameters are $s = \frac{1}{2}$, $a_\mathrm{b} = 0.2AU$, $q = 1$ and $f = 1$.

figures/f5/f5-eps-converted-to.pdf

Figure 5: Similar to Figure 4, but for different values of the binary mass ratio, as labeled.labeled. The input parameters are $s = \frac{1}{2}$, $s = \frac{1}{2}$, $a_\mathrm{b} = 0.2AU$, $\alpha = 0.01$ and $f = 1$.
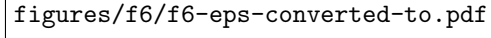
figures/f6/f6-eps-converted-to.pdf

Figure 6: Similar to Figure 4, but for different values of the binary torque coefficient f, as labeled. The input parameters are $s = \frac{1}{2}$, $a_{\rm b} = 0.2$ AU, $\alpha = 0.01$ and $q = 1$.
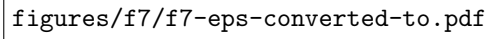
figures/f7/f7-eps-converted-to.pdf

Figure 7: temperature exponent effect.

figures/f8/f8-eps-converted-to.pdf

Figure 8: On the top left-hand panel, surface density profile of a disk orbiting a binary with a total mass $M_c = 1 \, \mathrm{M}_\odot$ and mass ratio $q = 1$ is shown for different times, as labeled. Solid and dashed curves are corresponding to the cases with the external and the internal winds, respectively. The adopted input parameters are $s = \frac{1}{2}$, $\alpha = 0.01$, $f = 1.0$, and $a_\mathrm{b} = 0.2\mathrm{AU}$. On the top right-hand panel, disk radius as a function of time is shown. On the bottom row, profiles of the disk mass (left) and evolutionary track in the plane of disk mass and radius (right) are shown for the presented solutions.

References

F. C. Adams, D. Hollenbach, G. Laughlin, and U. Gorti. Photoevaporation of Circumstellar Disks Due to External Far-Ultraviolet Radiation in Stellar Aggregates. , 611:360–379, aug 2004. doi: 10.1086/421989.

R. Alexander. The Dispersal of Protoplanetary Disks around Binary Stars. , 757:L29, oct 2012. doi: 10.1088/2041-8205/757/2/L29.

R. D. Alexander, C. J. Clarke, and J. E. Pringle. Photoevaporation of protoplanetary discs - II. Evolutionary models and observable properties. , 369:229–239, jun 2006. doi: 10.1111/j.1365-2966.2006.10294.x.

K. R. Anderson, F. C. Adams, and N. Calvet. Viscous Evolution and Photoevaporation of Circumstellar Disks Due to External Far Ultraviolet Radiation Fields. , 774:9, sep 2013. doi: 10.1088/0004-637X/774/1/9.

P. J. Armitage. Dynamics of Protoplanetary Disks. , 49:195–236, sep 2011. doi: 10.1146/annurev-astro-081710-102521.

P. J. Armitage and P. Natarajan. Accretion during the Merger of Supermassive Black Holes. , 567:L9–L12, mar 2002. doi: 10.1086/339770.

Steven A. Balbus and John F. Hawley. A powerful local shear instability in weakly magnetized disks. I - Linear analysis. II - Nonlinear evolution. *The Astrophysical Journal*, 376:214, jul 1991. doi: 10.1086/170270. URL https://doi.org/10.1086%2F170270.

R. D. Blandford and D. G. Payne. Hydromagnetic flows from accretion discs and the production of radio jets. , 199:883–903, jun 1982. doi: 10.1093/mnras/199.4.883.

L. R. Doyle, J. A. Carter, D. C. Fabrycky, R. W. Slawson, S. B. Howell, J. N. Winn, J. A. Orosz, A. Prša, W. F. Welsh, S. N. Quinn, D. Latham, G. Torres, L. A. Buchhave, G. W. Marcy, J. J. Fortney, A. Shporer, E. B. Ford, J. J. Lissauer, D. Ragozzine, M. Rucker, N. Batalha, J. M. Jenkins, W. J. Borucki, D. Koch, C. K. Middour, J. R. Hall, S. McCauliff, M. N. Fanelli, E. V. Quintana, M. J. Holman, D. A. Caldwell, M. Still, R. P. Stefanik, W. R. Brown, G. A. Esquerdo, S. Tang, G. Furesz, J. C. Geary, P. Berlind, M. L. Calkins, D. R. Short, J. H. Steffen, D. Sasselov, E. W. Dunham, W. D. Cochran, A. Boss, M. R. Haas, D. Buzasi, and D. Fischer. Kepler-16: A Transiting Circumbinary Planet. *Science*, 333:1602, sep 2011. doi: 10.1126/science.1210923.

B. Ercolano and I. Pascucci. The dispersal of planet-forming discs: theory confronts observations. *Royal Society Open Science*, 4:170114, apr 2017. doi: 10.1098/rsos.170114.

U. Gorti, C. P. Dullemond, and D. Hollenbach. Time Evolution of Viscous Circumstellar Disks due to Photoevaporation by Far-Ultraviolet, Extreme-Ultraviolet, and X-ray Radiation from the Central Star. , 705:1237–1251, nov 2009. doi: 10.1088/0004-637X/705/2/1237.

D. Hollenbach, D. Johnstone, S. Lizano, and F. Shu. Photoevaporation of disks around massive stars and application to ultracompact H II regions. , 428:654–669, jun 1994. doi: 10.1086/174276.

M. Li and L. Xiao. Lifetimes and Accretion Rates of Protoplanetary Disks. , 820:36, mar 2016. doi: 10.3847/0004-637X/820/1/36.

D. Lynden-Bell and J. E. Pringle. The evolution of viscous discs and the origin of the nebular variables. , 168:603–637, sep 1974. doi: 10.1093/mnras/168.3.603.

A. I. MacFadyen and M. Milosavljević. An Eccentric Circumbinary Accretion Disk and the Detection of Binary Massive Black Holes. , 672:83–93, jan 2008. doi: 10.1086/523869.

R. G. Martin, P. J. Armitage, and R. D. Alexander. Formation of Circumbinary Planets in a Dead Zone. , 773:74, aug 2013. doi: 10.1088/0004-637X/773/1/74.

J. A. Orosz, W. F. Welsh, J. A. Carter, D. C. Fabrycky, W. D. Cochran, M. Endl, E. B. Ford, N. Haghighipour, P. J. MacQueen, T. Mazeh, R. Sanchis-Ojeda, D. R. Short, G. Torres, E. Agol, L. A. Buchhave, L. R. Doyle, H. Isaacson, J. J. Lissauer, G. W. Marcy, A. Shporer, G. Windmiller, T. Barclay, A. P. Boss, B. D. Clarke, J. Fortney, J. C. Geary, M. J. Holman, D. Huber, J. M. Jenkins, K. Kinemuchi, E. Kruse, D. Ragozzine, D. Sasselov, M. Still, P. Tenenbaum, K. Uddin, J. N. Winn, D. G. Koch, and W. J. Borucki. Kepler-47: A Transiting Circumbinary Multiplanet System. *Science*, 337:1511, sep 2012. doi: 10.1126/science.1228380.

J. E. Owen, B. Ercolano, C. J. Clarke, and R. D. Alexander. Radiation-hydrodynamic models of X-ray and EUV photoevaporating protoplanetary discs. , 401:1415–1428, jan 2010a. doi: 10.1111/j.1365-2966.2009. 15771.x.

J. E. Owen, B. Ercolano, C. J. Clarke, and R. D. Alexander. Radiation-hydrodynamic models of X-ray and EUV photoevaporating protoplanetary discs. , 401:1415–1428, jan 2010b. doi: 10.1111/j.1365-2966.2009. 15771.x.

J. E. Owen, B. Ercolano, and C. J. Clarke. Protoplanetary disc evolution and dispersal: the implications of X-ray photoevaporation. , 412:13–25, mar 2011a. doi: 10.1111/j.1365-2966.2010.17818.x.

J. E. Owen, B. Ercolano, and C. J. Clarke. Protoplanetary disc evolution and dispersal: the implications of X-ray photoevaporation. , 412:13–25, mar 2011b. doi: 10.1111/j.1365-2966.2010.17818.x.

F. I. Pelupessy and S. Portegies Zwart. The formation of planets in circumbinary discs. , 429:895–902, feb 2013. doi: 10.1093/mnras/sts461.

G. P. Rosotti and C. J. Clarke. The evolution of photoevaporating viscous discs in binaries. , 473:5630–5640, feb 2018. doi: 10.1093/mnras/stx2769.

M. E. Schwamb, J. A. Orosz, J. A. Carter, W. F. Welsh, D. A. Fischer, G. Torres, A. W. Howard, J. R. Crepp, W. C. Keel, C. J. Lintott, N. A. Kaib, D. Terrell, R. Gagliano, K. J. Jek, M. Parrish, A. M. Smith, S. Lynn, R. J. Simpson, M. J. Giguere, and K. Schawinski. Planet Hunters: A Transiting Circumbinary Planet in a Quadruple Star System. , 768:127, may 2013. doi: 10.1088/0004-637X/768/2/127.

N. I. Shakura and R. A. Sunyaev. Black holes in binary systems. Observational appearance. , 24:337–355, 1973.

D. Vartanyan, J. A. Garmilla, and R. R. Rafikov. Tatooine Nurseries: Structure and Evolution of Circumbinary Protoplanetary Disks. , 816:94, jan 2016. doi: 10.3847/0004-637X/816/2/94.

L. Xiao and Q. Chang. Evolution and Photoevaporation of Protoplanetary Disks in Clusters: The Role of Pre-stellar Core Properties. , 853:22, jan 2018. doi: 10.3847/1538-4357/aa9ff1.